Title

Electronic surface reconstruction of TiO2 nanocrystals revealed by resonant inelastic x-ray scattering

Journal

Journal of Vacuum Science & Technology A Vacuum Surfaces and Films, 39(6)

ISSN

0734-2101

Authors

Chuang, Cheng-Hao
Chen, Chieh-Ming
Shao, Yu-Cheng
et al.

Publication Date

2021-12-01

DOI

10.1116/6.0001247

Peer reviewed

Electronic Surface Reconstruction of TiO_2 Nanocrystals Revealed by Resonant Inelastic X-ray Scattering

Cheng-Hao Chuang

Department of Physics, Tamkang University, Tamsui 251, New Taipei City, Taiwan

Advanced Light Source, Lawrence Berkeley National, Laboratory, Berkeley, California 94720, USA

Chieh-Ming Chen, Yu-Cheng Shao, Ping-Hung Yeh, Chih-Ming Chang, and Way-Faung Pong

Department of Physics, Tamkang University, Tamsui 251, New Taipei City, Taiwan

Mukes Kapilashrami and Per-Anders Glans

Advanced Light Source, Lawrence Berkeley National Laboratory, Berkeley, California 94720, USA

Sheraz Gul, Gongming Wang, Yat Li, and Jin Zhang

Department of Chemistry and Biochemistry, University of California, Santa Cruz, California 95064, USA

Jun Miyawaki, Hideharu Niwa, and Yoshihisa Harada

The institute for Solid State Physics, The University of Tokyo, Kashiwanoha, Kashiwa, Chiba 277-8526, Japan

Jin-Ming Chen

National Synchrotron Radiation Research Center, Hsinchu 300, Taiwan

Jinghua Guo *

Advanced Light Source, Lawrence Berkeley National Laboratory, Berkeley, California 94720, USA and

Department of Chemistry and Biochemistry, University of California, Santa Cruz, California 95064, USA

Abstract

The identification for lattice multiphases in TiO_2 nanocrystals is studied by high resolution transmission electron microscope and electron diffraction pattern. Based on the spectroscopic analysis using soft X-ray absorption and resonant inelastic soft X-ray scattering, it is believed that the oxygen vacancies at the interface exhibit the structural distortion of TiO_6^{8-} cluster around the defect site as for the multiphase lattice. We elucidate that the extra 3*d* electrons nearby induce the inelastic scattering features with the excitation-energy dependence owing to different energy relaxation processes, characteristic of the electron-phonon coupling or nature of electron-hole pair at the intermediate state. The manifold *dd* excitations driven by the strong interaction between Ti-3*d* and O-2*p* electrons is noticeably rich co-existed on both Ti and O sites. The sophisticated experiment can advance the perspective of nano-composite TiO_2 for various interactions of surface Ti^{3+} in the application of future devices.

Keywords: soft X-ray, XAS, RIXS, TiO_2 nanocrystals

* Author to whom correspondence should be addressed: jguo@lbl.gov

I. INTRODUCTION

Ti-O nanocomplexes are one of the most widely studied photoactive semiconductor materials owing to their inherently-chemical stability, readily availability, tunable electronic properties, and non-toxicity.[1,2] Among these, the three polymorphys of TiO_2 (rutile, anatase, and brookite phases) with a bandgap ranging from 3.0 to 3.2 eV are commonly appropriate for the photoelectric properties in the ultraviolet (UV) wavelength region and succeeding application e.g. photocatalysis,[3] biosensors,[4] and photo-electrochemical cells.[5] In the quest of enhancing the photoelectric effect, it is crucial to understand how to impact the related electronic properties of the oxide, such as the role of lattice defects (e.g. oxygen vacancies) and introduction of impurity elements into the host oxide matrix (a.k.a. doping) towards the alteration of its intrinsic properties.[2] Generally, oxygen vacancies give rise to the mid-gap states (typically located close above or below the valence band maximum and conduction band minimum, respectively) serving as active charge trapping states and thus impeded the photoelectric effect by accelerating the electron-hole recombination rate.[6] The discussion for this kind of lattice and electronic correlation is often seen in the oxide, but so far the comprehensive insight for the nanoscale dimension is lack.

Titanium dioxide of trivalent Ti configuration (Ti^{3+}) is a strongly correlated transition metal oxide with the complex correlation of both occupied and unoccupied states.[7] While the presence of trivalent Ti on the surface of TiO_2 nanocomplexes have previously been reported,[8,9] the role at inter-surface levels remains to be fully understood for the Ti-O interaction. However, difficulties in identifying these Ti^{3+} species, typically embedded at the interface between a disordered ”nanophase” precipitated on the surface of an otherwise crystalline core, is often conducted by combined electron microscopy (e.g. scanning tunnel microscopy and/or transmission electron microscopy (TEM)) and X-ray photoelectron spectroscopy (XPS) studies to emanate details on the surface and subsurface geometry, chemical state, valence band (VB) and lattice structure of the oxide.[10,11] For all that, these experimental capabilities do not shed light on the element-specific contribution to localized electron-hole recombination sites, nor relating the specific strong correlation between Ti and O sites in the case of closing to the Fermi level.

In this connection, we present herein combined high resolution transmission electron microscopy and detailed soft X-ray spectroscopy (namely *X-ray Absorption Spectroscopy* (XAS) and *Resonant Inelastic X-ray Spectroscopy* (RIXS)) studies on the electronic properties of TiO_2 nanocrystals (NCs) - specifically the correlation between trivalent Ti and local charge symmetry on the surface at inter-surface levels. XAS and RIXS represents two key spectroscopy techniques, probing the element-related information in the unoccupied and occupied state near the Fermi level under resonant utilization.[12,13] As to the excitors, the insight for the energy- and momentum-losses between incident and emitted X-ray could illustrate the underlaying mechanism of energy transfer, charge separation, phonon interference, and orbital hybridization,[12,14] since the losses are considered to have the new decaying paths (for certain energy/momentum transfer) acting as the excited electron-hole pair in the intermediate state, being forecast for the following Ti^{3+} identification. As at and above resonant absorbance, the emission dispersion of RIXS is strongly dependent on the inter- and intra-correlation between charge, spin, lattice, and orbital, also defined as resonant X-ray emission spectroscopy (RXES). We present herein detailed XAS and RIXS measurement on the structural and electronic properties of intrinsic TiO_2 NCs composed of a crystalline core and an amorphous surface, in particular for the role of Ti^{3+} state.

II. RESULTS

High resolution TEM studies revealed existence of clusters of TiO_2 NCs with ordered lattice fringes and lattice planes, *ca.* 0.184 and 0.285 nm apart (Fig. 1a). Fig. 1b presents the select area electron diffraction (SAED) along the (001) and (202) planes (collected across the entire surface area of the particle). The point of view confirms that TiO_2 NCs are predominantly composed of an anatase phase.[15] Besides, it occurs the diffraction rings at the center, typically telling the presence of multiphase-typed lattice (i.e. the amorphous phases), because a large number of randomly oriented grains results in the merged spots extensively seen as circle rings. The darker region on the surface in Fig. 1a renders it possible for the multiphase region. The statistical analysis of various TiO_2 NCs indicates that the ratio of darker region (amorphous area) is 42.4% relative to the area of whole NCs; thus, the next matter is how to identify it by spectroscopic

perspective, such as the structural defect and multiphase formation. The element-specific spectroscopy is employed for the multiphase (amorphous) contribution further.

The element-sensitive XAS technique, monitoring the transition intensity from a core electron to the unoccupied density of states, is specific in the details of electronic structure, charge symmetry, and charge transition in complex materials. The Ti *L*-edge XAS in Fig. 2a reflects the Ti $2p \rightarrow 3d$ transitions (TiO_2 NCs and reference XAS spectra of anatase- and rutile-TiO_2). The features at photon energy 458.0 (463.2) eV, and 460.1 (465.2) eV are known as the multiples t_{2g} and e_g of Ti 3*d* orbitals in L_3 (L_2) edge,[16] because ligand-field splitting in the octahedral complexes of TiO_2 (Ti^{4+} configuration) denotes the unfilled t_{2g} (*xy*, *yz*, and *yz*) and e_g (x^2-y^2 and z^2) symmetries. The e_g sub-band segregated from TiO_6^{8-} ligand field is denoted as the driving force to split the peak (459.7 and 460.6 eV), which making two-phase (anatase- and rutile-TiO_2) recognizable. Fig. 2b presents the O *K*-edge XAS spectra from O $1s \rightarrow 2p$ transitions in the TiO_2 samples. Spectral features at 530.7 and 533.2 eV are derived from O 2*p* states coupled to Ti 3*d* (i.e. t_{2g} and e_g sub-bands), whereas the spectral features in the higher energy range can be assigned to O 2*p*-Ti 4*s* (at 538.9 eV) and O 2*p*-Ti 4*p* (at 544.5 eV) hybridization, respectively.[2,17] The absorption spectra (Ti *L*-edge and O *K*-edge) of TiO_2 NCs show a similar anatase phase by the bulk reference, which is well in line with our findings from HRTEM studies (see Fig. 1b). However, absorption features seem no obvious difference in TiO_2 NCs and bulk reference. Thus, the other investigation is demanded to seek for the odd multiphase on the interface, such like the hetero-NCs (core/shell for Ti^{4+}/Ti^{3+}), as being lower spectral Ti^{3+} weight.[6]

X-ray emission spectroscopy (XES) measures the recombination intensity from the electron in VB/CB to the core hole obeying the energy and momentum conservation. On/off resonant condition by the incident X-ray energy makes the intermediate states different in the de-excitations process, which is utilized for small amount distinction of multiphase complex system.[12,13] RIXS spectra at Ti *L*-edge and O *K*-edge, respectively, have been acquired at the excitation energies (indicated at A-I and A'-H' in Fig. 2). The RIXS spectral features at Ti *L*-edge in Fig. 3a reflect: (i) elastic scattering, (ii) fluorescence emission, and (iii) inelastic scattering in the energy-loss axis. The sharp peak at the high-energy side (i), which follows the incident X-ray energies as the Rayleigh scattering, is used to calibrate the emission energy scale.

As evident for (ii), the energy position of the broad peak centered at *ca.* 450.0 eV does not change notably with the increased excited photon energies, which can be explained by the constant energy difference between the VB and the core-level state of Ti site. The RIXS spectra in Fig. 3b indicate that the energy-loss profiles (iii) in the energy interval *ca.* 4 to 0 eV are attributed to the inelastic scattering features. Excited at photon energies for the unoccupied t_{2g} and e_g state (A-I), the asymmetric shaped tail arises its intensity and grows the multi-features nearby. Resonant along Ti $3d^1$-t_{2g} peak (A-C), a growing peak at 0.9 eV starts to move its energy-loss position up to 1.5 eV above the asymmetric tail. At the valley between the t_{2g} and e_g state (E), double-peak shows up at energy-loss position at 1.1 and 2.6 eV. As exciting at higher energy (F-H for Ti $3d^1$-e_g), the first (second) peak shifts from 1.1 (2.6) to 1.8 (2.9) eV with the incident energy dependence. It is similar to the de-excitation process (from A to D) around the resonant absorption of Ti $3d^1$-t_{2g} state. In fact, the RIXS of anatase and rutile TiO_2 ($3d^0$ configuration) have previously manifested absence of *dd* excitations,[18,19] as the $\underline{c}3d^1$ RIXS intermediate states do not give rise to the electron-electron scattering (*dd* excitations). The present inelastic features in the energy interval *ca.* 4 to 0 eV are in agreement with the *dd* excitations assignment in Li_xTiO_2 (x=0 ~ 0.5 for $3d^0 \rightarrow 3d^1$ configuration) and core-shall TiO_2 nanowire for the inter-transition (t_{2g}-t_{2g}) and intra-transition (t_{2g}-e_g) of Ti site.[6,18] It is generally admitted that an ideal scheme to interpret the excitation-dependent shift of inelastic peaks and asymmetric part of elastic peak is essential to do the theoretical calculation (i.e density functional theory). On the other hand, the shift of *dd* excitations with the scan of absorption energy in our TiO_2 NCs is analogous to Moser *et al*[20] result, describing the coexistence of delocalized *dd* feature and asymmetric tail happened at the transition to Ti e_g orbitals is derived from the poorly screened core hole and more delocalized e_g states.[21] Thus, RIXS result of TiO_2 NCs denotes the spectroscopic measurement toward the structural transition between the surface (Ti^{3+} states) and core (Ti^{4+} states).

Fig. 3d and 3e display the O *K*-edge RIXS spectra at excitation energy of 529.5 to 533.2 eV in the emission energy and energy-loss representation. The main feature, centered at *ca.* 525.7 eV, projects the *partial density of states (pDOS)* in the VB mixing of O 2*p* and Ti 3*d* orbitals.[18] At the resonant energy point (E'), an additional energy-loss feature at 1.4 eV emerges from the asymmetric sideband. Moving to the higher energy point (F'), it grows double features up at 1.5 eV and 2.2 eV. To emphasize the asymmetric weight among the energy-loss range of 0 to 3 eV,

the spectral difference analysis, by subtracting the symmetric shape of the elastic peak (pre-edge absorption, A') from each of asymmetric profiles, is exhibited in Fig. 3f. At the resonances of O 2*p* and Ti 3*d*-t_{2g} state (B'-A' to E'-A'), the raising positive signal (the increasing asymmetric part from the elastic peak) is shown in the range of 0 to 3 eV, while the absorption and de-excitation process are assumed to vibrate the core-level state, as the step to increase the energy relaxation. Probing at the off-resonant energy point, the difference spectra (F'-A' and G'-A') has the slight difference in the range of 0 to 1 eV, but there is a new wide peak in the region of 1 to 3 eV. At absorption peak (H'), the asymmetric sideband with a long tail is found again by the strong relaxation process at the resonant O 2*p* and Ti $3d^1$-e_g. Apparently, the increasing asymmetric tail with the confident peak is expanded from the symmetric center of the elastic-scattering matter. It is similar to the previous case of graphite for the lattice distortion around excited carbon atoms as a "long-tail" towards the low-energy side.[22]

Fig. 4a shows a comparison for both Ti and O RIXS spectra. For the excitation below O 2*p* and Ti $3d^1$-t_{2g} hybridized state, the RIXS profile (A) at the Ti site reveals the *dd* excitation (t_{2g}-t_{2g}) and electron decay channel, while the profile (A') at O site reflects only the symmetric elastic scattering. At the resonance to the O 2*p* and Ti $3d^1$-t_{2g} hybridized state, RIXS feature at Ti site (C) has one broad peak around 1.5 eV on the asymmetric sideband, similar to that of O K_α emission (E'). Just above this resonance (E for Ti; G' for O), one mixing *dd* excitations at 2.3 eV is present at the O site while the split features are probed at the Ti site. Upon resonant excitation to the O 2*p* and Ti $3d^1$-e_g hybridized state (H and H'), the RIXS profiles in both sites reveal the asymmetric tail but *dd* excitation is visible only for Ti. So far, no inelastic decay features (inelastic relaxation and *dd* excitations) have been previously reported in the O K_α RIXS spectra of TiO_2 even in the Ti $3d^1$ configuration.[18,20] While we consider the lifetime of the electronic core-hole state (intermediate state), which is long enough by the resonant condition to allow the atoms to move suffered from the mixing coordination of normal Ti^{4+} and vacant Ti^{3+} site (i.e. phonon relaxation), the emission spectra have the chance to observe a long tail extending from the elastic state (shown as asymmetric shoulder).[22,23] It comes to the decaying channels being different vibrational energy levels or specific nature of unoccupied state of TiO_2 NCs; most of all, the RIXS measurement displays a long energy-loss tail and two shifted peaks (*dd* excitations) *via* the electron-electron couplings and defect induced multiphase coordination.

In Fig. 4b, XPS-VB (hv = 150.0 eV), oxygen K-edge NXES (hv = 570.0 eV), and RIXS (hv = 530.7 eV (E')) spectra are aligned for the element-related comparison. The oxygen NXES reflects the *partial density of states (pDOS)* of VB, where the valence band maximum is located at BE 3.7 eV in XPS-VB measurement. The XPS-VB spectrum (denoted as *total* DOS) in inset of Fig. 4b discloses one peak at BE 1.4 eV within the bandgap region, which is absent in oxygen NXES (*pDOS*).[7,24] As probing at resonant state (hv = 530.7 eV (E')), the spectral feature (around energy-loss position 0 and 3 eV) grows up within the bandgap region of TiO_2 NCs, mostly corresponding to the Ti $3d^1$-t_{2g} hybridizing to O $2p$. In other words, the absence of oxygen-related electron in VB range is evaluated by the *pDOS* measurement of oxygen K-edge NXES. The hybrid state between the extra Ti-$3d^1$ electrons and O $2p$ valence state though the Ti-O coupling is verified by the *total* DOS measurement of XPS-VB data and resonant features of RIXS data. Thus, Fig. 3c draws the lattice coordination of TiO_2 NCs, where oxygen vacancies introduce lattice distortion and delocalized $3d$ elections within the TiO_6^{8-} clusters. The Ti^{3+} site with lattice *expansion* and O/Ti^{4+} sites with lattice *compression* (from the on-site Coulomb interactions) are shown. After the on-resonant enhancement and multiphase-induced Ti^{3+} state (t_{2g} and e_g), the collective movement around the oxygen vacancy makes the nearby Ti/O sites coordinative well, playing as a new decay channel (asymmetric tail).

The relevant aspects for the intermediate state selected at Ti and O site by RIXS is shown in Fig. 5a. The Ti $2p$ electron is excited to the unoccupied $3d^1$-t_{2g} orbital in the absorption process, then the core hole and excited electron as the intermediate state yields the perturbation around the oscillated lattice and $3d$ excitation in case of the strong Coulomb interaction and less screen effect. The inter dd excitation in the Ti L-edge RIXS is ascribed to the Ti $3d^1$-t_{2g} orbital of multi-phase TiO_2 NCs with the intensive electron-electron interactions. Fig. 5b illustrates that the inelastic scattering process on O site forms the inter dd transition of Ti $3d^1$ electron *via* the strong Ti and O orbital hybridization. On the contrary, RIXS at O $2p$ and Ti $3d^1$-e_g hybridized state doesn't induce the $3d$ electron-electron interaction due to no d-electron in the Ti-e_g state and lower heterogeneous O and Ti coupling. The excitation-energy dependence of RIXS highlights the role of Ti $3d^1$-t_{2g} electron in the TiO_2 NCs.

III. METHODS

NCs of intrinsic TiO_2 were synthesized through sol-gel method in which metal alkoxide $Ti(OR)_4$ precursor was used. Titanium tetraisopropoxide (TTIP) (97%, Aldrich) was mixed with a solution of ethanol (99.5%, Aldrich) and HCl (37%) for stirring an hour. The next step was added to the mixture of water and polyethylene glycol (7% PEG, Aldrich) to form the hydrophilic group at interface. TiO_2 NCs of average particle size 100 nm were spin coated on fluorine-doped tin oxide substrates and annealed at 530°C (post deposition) under ambience condition for 1 hour.[25,26] The local structural symmetry and atomic arrangement was confirmed by high resolution TEM (JEOL-2100F-HR TEM) studies including select area diffraction (SAED) pattern. Ti *L*-edge and O *K*-edge XAS spectra have been recorded in the surface sensitive (probing depth $\sim$ $\lesssim$ 10 nm) total electron yield (TEY) detection mode at beamline(s) 7.3.1 and 8.0.1.4 at Advanced Light Source (ALS) and beamline 20A at National Synchrotron Radiation Research Center (NSRRC). Furthermore, to better resolve the electron-correlated phenomena, RIXS spectra were recorded at beamline 7.0 LSU at SPring-8, Japan (with a combined monochromator and spectrometer resolution $\sim$ $\lesssim$ 0.12 eV at Ti *L*-edge).[27]

IV. CONCLUSION

In summary, the core/shell interface of TiO_2 NCs is found to be composed of both nanocrystalline with Ti^{4+} species and amorphous phase with Ti^{3+} species. The oxygen vacancy serves as the dilute Ti^{3+} state, thus the decay channels of Raman excitations become noticeable. Each anion vacancy introduces two unbonded $3d^1$ electrons at the defect center, which is manifested by the single/double-peak excitations at non-constant energy loss (delocalized 3d character) and is connected to the t_{2g}-π bound and collective lattice movement. Through the π bonding for Ti $3d^1$ state, the delocalized excitations of $3d^1$ carrier are corresponding to the electron hopping movement among oxygen vacancy. The strong correlation of Ti-3*d* and O-2*p* orbitals induces energy transfer between t_{2g} and e_g. The electron-phonon coupling of the core exciton state is sensitive to the lattice distortion around Ti and O atoms. The two phases (Ti^{3+} and Ti^{4+}) in TiO_2 nanocomposite constitutes the unambiguous electron-phonon (asymmetric sideband) and electron-electron (localized and delocalized *dd* excitations) coupling. This

investigation provides an alternative understanding for the correlated 3*d* electrons generated by the oxygen vacancy of nanoscale dimension.

V. ACKNOWLEDGMENTS

This research was supported by the Ministry of Science and Technology, Taiwan (MOST) (MOST 1042112-M-032-005-MY2). RIXS experiments were carried jointly by the University of Tokyo (Proposal No. 2012A7428, 2012B7438, 2013A7450). This research used resources of the Advanced Light Source, a U.S. DOE Office of Science User Facility under contract no. DE-AC02-05CH11231. MK acknowledges DOE funding support under Contract No. DE-SC0006931.

VI. COMPETING INTERESTS

The authors declare that they have no competing financial interests

VII. DATA AVAILABILITY STATEMENT

The data that support the findings of this study are available from the corresponding author upon reasonable request.

VIII. REFERENCES

[1] M. Ni, M. K. H. Leung, D. Y. C. Leung, and K. Sumathy, *Renewable and Sustainable Energy Reviews* **11**, 401 (2007)

[2] M. Kapilashrami, Y. Zhang, Y.-S. Liu, A. Hagfelds, and J.-H. Guo, *Chem. Rev.* **114**, 9662 (2014).

[3] Q. Guo, C. Zhou, Z. Ma, X. Yang, *Adv. Mater.* **31**, 1901997 (2019).

[4] N. Khaliq, M. A. Rasheed, M. Khan, M. Maqbool, M. Ahmad, S. Karim, A. Nisar, P. Schmuki, S. Oh Cho, and G. Ali, *ACS Appl. Mater. Interfaces* **13**, 3653 (2021).

[5] P. A. Gross, N. Javahiraly, N. Geraldini Sabat, T. Cottineau, E. R. Savinova, and V. Keller, *Appl. Phys. Lett.* **109**, 153903 (2016).

[6] J. Li, C.-H. Liu, X. Li, Z.-Q. Wang, Y.-C. Shao, S.-D. Wang, X.-L. Sun, W.-F. Pong, J.-H. Guo, and T.-K. Sham, *Chem. Mater.* **28**, 4467 (2016).

[7] X. Chen, L. Liu, Z. Liu, M. A. Marcus, W.-C. Wang, N. A. Oyler, M. E. Grass, B. Mao, P.-A. Glans, J.-H. Guo, and S. S. Mao, *Scientific Reports* **3**, 1510 (2013).

[8] T. Minato, Y. Sainoo, Y. Kim, H. S. Kato, K. Aika, M. Kawai, J. Zhao, H. Petek, T. Huang, W.
He, B. Wang, Z. Wang, Y. Zhao, J. Yang, and J. G. Hou, *J. Chem. Phys* **130**, 124502 (2009).

[9] S. Wendt, P. T. Sprunger, E. Lira, G. K. H. Madsen, Z. Li, J. Hansen, J. Matthiesen, A. Blekinge-Rasmussen, E. Laegsgaard, B. Hammer, and F. Besenbacher, *Science* **320**, 1775 (2008).

[10] X. Chen, L. Liu, P. Y. Yu, and S. S. Mao, *Science* **331**, 746 (2011).

[11] J. Tao and M. Batzill, *J. Phy. Chem. Lett.* **1**, 3200 (2010).

[12] L. J. P. Ament, M. van Veenendaal, T. P. Devereaux, J. P. Hill, and J. van den Brink, *Rev. Mod. Phys.* **83**, 705 (2011).

[13] X. Feng, S. Sallis, Y.-C. Shao, R. Qiao, Y.-S. Liu, L. C. Kao, A. S. Tremsin, Z. Hussain, W. Yang, J.-H. Guo, and Y.-D. Chuang, *Phys. Rev. Lett.* **125**, 116401 (2020).

[14] P. Kuiper, J.-H. Guo, C. Sathe, L.-C. Duda, J. Nordgren, J. J. M. Pothuizen, F. M. F. de Groot, and G. A. Sawatzky, *Phys. Rev. Lett.* **80**, 5204 (1998).

[15] J. A. Chang, M. Vithal, I. C. Baek, and S. I. Seok, *J. Solid State Chem.* **182**, 749 (2009).

[16] C. X. Kronawitter, M. Kapilashrami, J. R. Bakke, S. F. Bent, C.-H. Chuang, W.-F. Pong, J.-H.
Guo, L. Vayssieres, and S. S. Mao, *Phys. Rev. B* **85**, 125109 (2012).

[17] L. Liu, J. Chan, and T.K. Sham, *Phys. Rev. B* **85**, 125109 (2012).

[18] A. Augustsson, A. Henningsson, S. M. Butorin, H. Siegbahn, J. Nordgren, and J.-H. Guo, *J. Chem. Phys.* **119**, 3983 (2003).

[19] Y. Harada, T. Kinugasa, R. Eguchi, M. Matsubara, A. Kotani, M. Watanabe, A. Yagishita, and S. Shin, *Phys. Rev. B* **61**, 12854 (2000).

[20] S. Moser, S. Fatale, P. Kru¨ger, H. Berger, P. Bugnon, A. Magrez, H. Niwa, J. Miyawaki, Y. Harada, and M. Grioni, *Phys. Rev. Lett.* **115**, 096404 (2015).

[21] K.-J. Zhou, M. Radovic, J. Schlappa, V. Strocov, R. Frison, J. Mesot, L. Patthey, and T. Schmitt, *Phys. Rev. B* **83**, 201402 (2011).

[22] Y. Harada, T. Tokushima, Y. Takata, T. Takeuchi, Y. Kitajima, S. Tanaka, Y. Kayanuma, and S. Shin, *Phys. Rev. Lett.* **93**, 017401 (2004).

[23] S. Eisebitt and W. Eberhardt, *J. Electron. Spectrosc. Related. Phenom.* **110-111**, 335 (2000).

[24] M. Batzill, E. H. Morales, and U. Diebold, *Phys. Rev. Lett.* **96**, 026103 (2006).

[25] B. Guo, Z. Liu, L. Hong, H. Jiang, J. Y. Lee, *Thin Solid Films* **479**, 310 (2005).

[26] G. Wang, H. Wang, Y. Ling, Y. Tang, X. Yang, R. C. Fitzmorris, C. Wang, J. Z. Zhang, and Y. Li, *Nano Lett.* **11**, 3026 (2011).

[27] Y. Harada, M. Kobayashi, H. Niwa, Y. Senba, H. Ohashi, T. Tokushima, Y. Horikawa, S. Shin, and M. Oshima, *Rev. Sci. Instrum.* **83**, 013116 (2012).

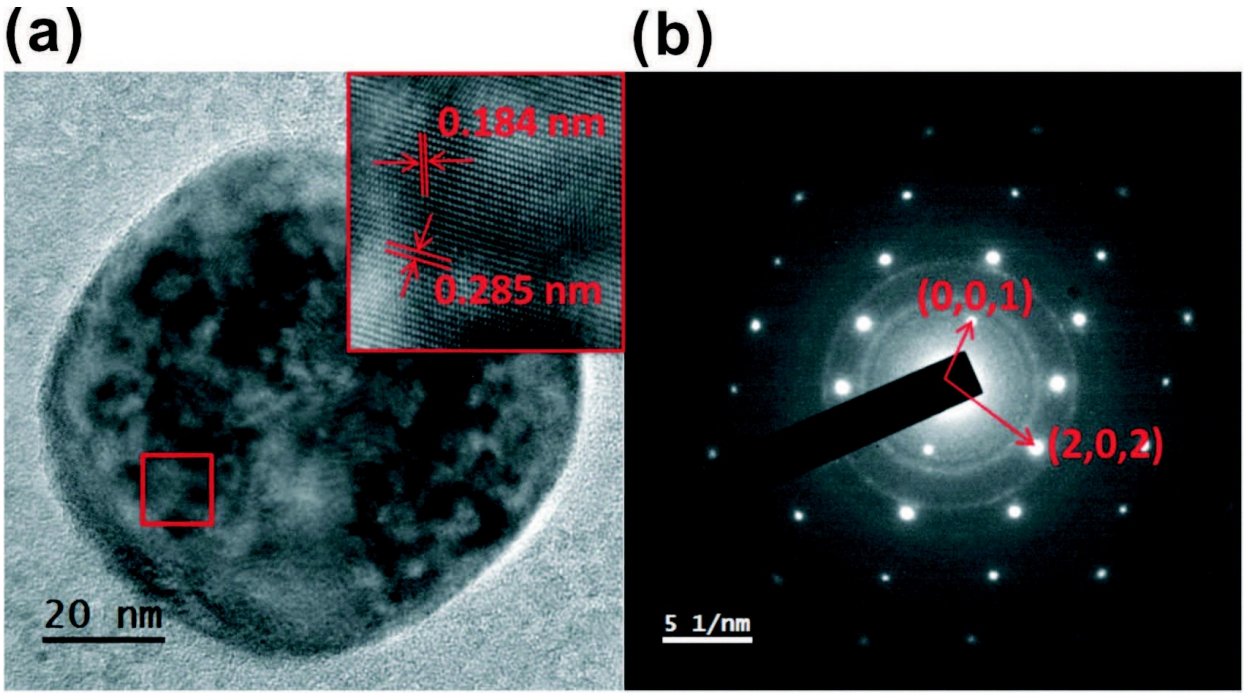

FIG. 1: (a) TEM image of TiO_2 NCs indicating clusters of ordered lattice fringes and planes *ca.* 0.184 and 0.285 nm apart. (b) Typical SAED pattern indicating a multiphase (mixing amorphous + crystalline) lattice as evidence from combined the diffraction spots and circles.

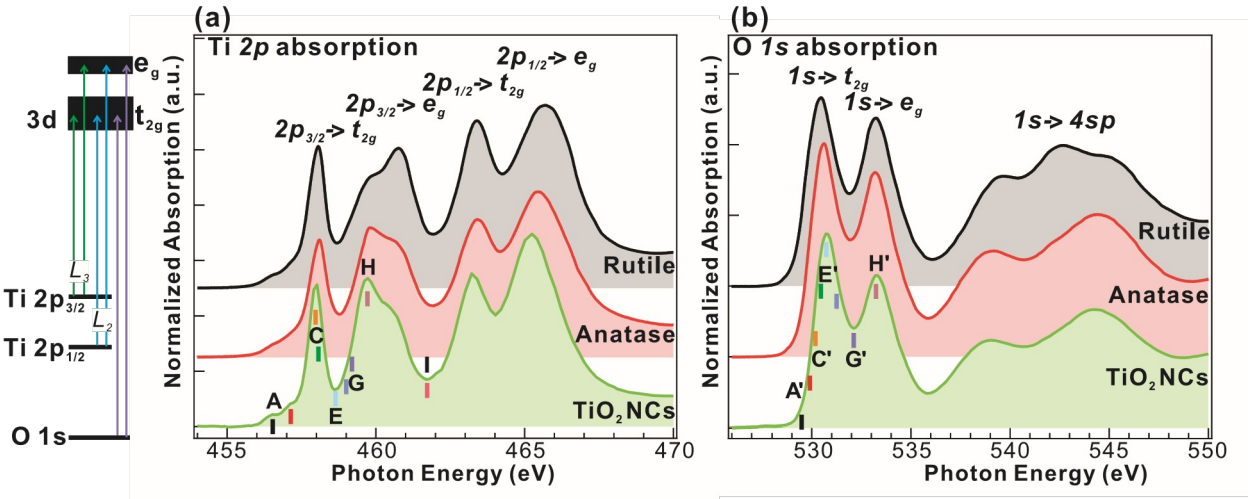

FIG. 2: Comparison of the absorption spectra of anatase, rutile, TiO_2 NCs: (a) Ti $L3,_2$-edge (a) and O *K*-edge.

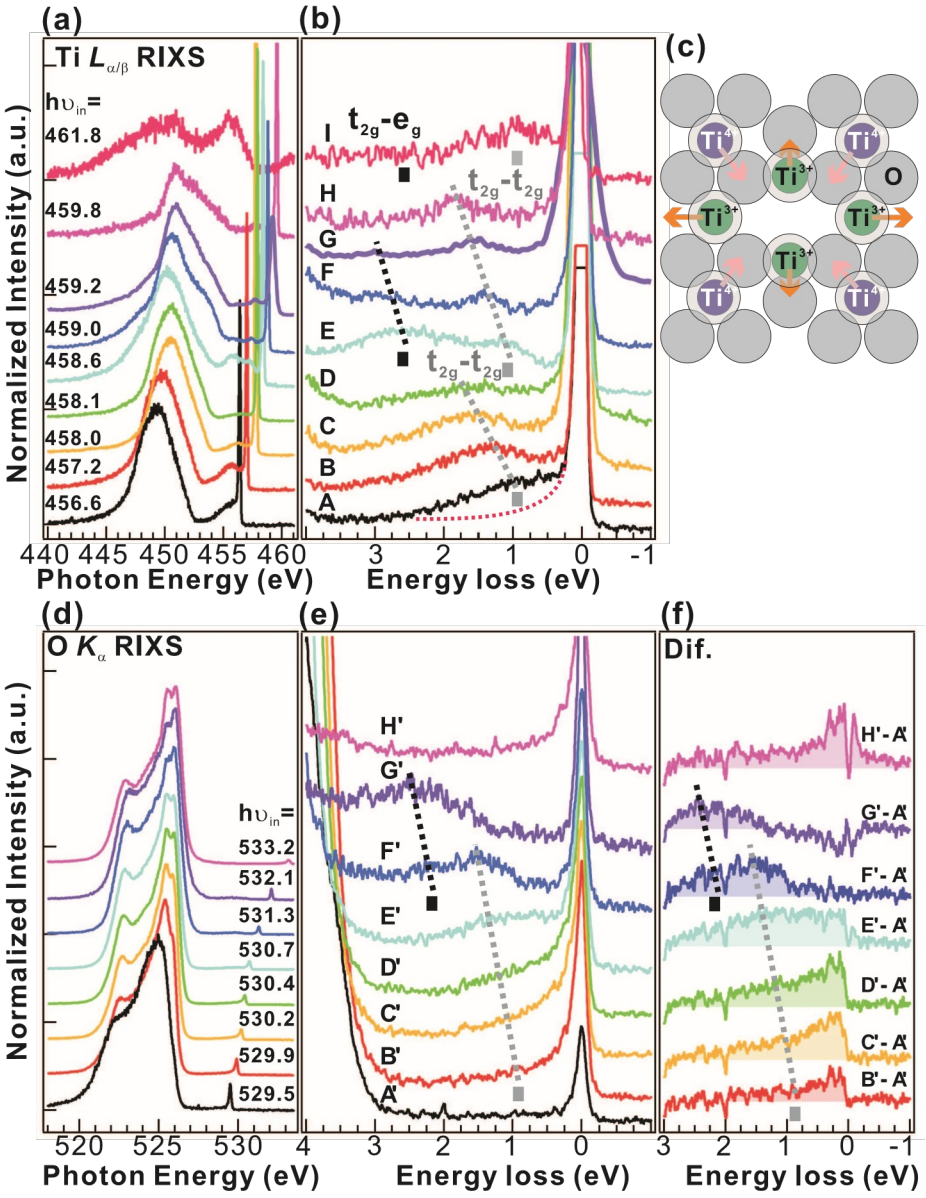

FIG. 3: (a) and (d) Ti $L_{\alpha/\beta}$ and O K_{α} RIXS spectra of TiO_2 NCs. (b) and (e) in energy-loss scale. The delocalized *dd* excitations are found around the range of 0 to 4 eV, and the electron-phonon coupling appears in the asymmetric tail of elastic state. The presenation of (f) is the difference spectra from the elastic scattering one (A') to inelastic latter one (B' ~ H'). Scheme of (c) oxygen vacancy induced structural distortion.

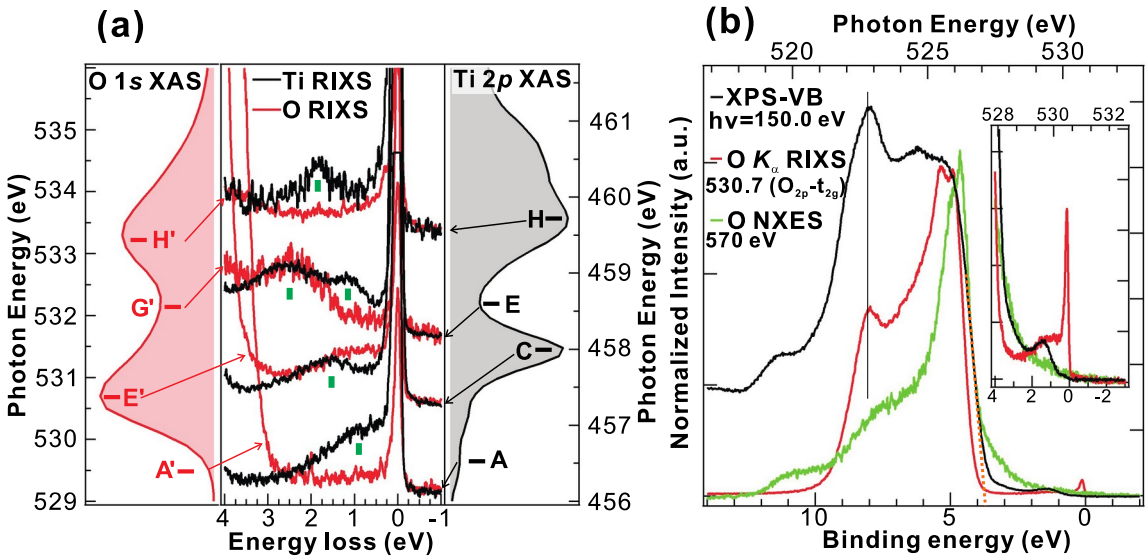

FIG. 4: (a) The emission comparison of on-and off-resonant RIXS measured in Ti and O site. (b) Valence band and O K_α RIXS spectra of TiO_2 NCs.

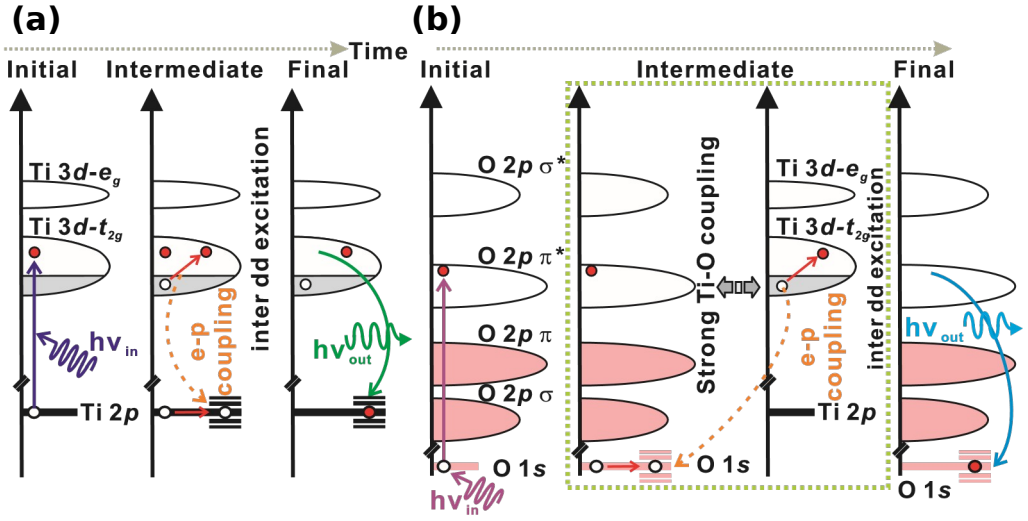

FIG. 5: (a) and (b) various d-d excitations models probed by the elastic scattering from Ti and O site, individually.